Journal of Otology 19 (2024) 133–139

Contents lists available at ScienceDirect

Journal of Otology

journal homepage: www.journals.elsevier.com/journal-of-otology/

Loss of Fascin2 increases susceptibility to cisplatin-induced hearing impairment and cochlear cell apoptosis in mice

Yan Wang [a,1], Yingying Liu [a,1], Yi Xie [a], Jun Luan [a], Rongrong Liu [a], Yongjia Zhu [a], Ying Ma [a], Yi Fan [a], Yan Sun [b], Wenjing Shang [a,**], Fengchan Han [a,*]

[a] Department of Biochemistry and Molecular Biology, and Key Laboratory for Genetic Hearing Disorders in Shandong, Binzhou Medical University, 346 Guanhai Road, Yantai, 264003, Shandong, PR China
[b] Department of Otorhinolaryngology-Head and Neck Surgery, Affiliated Yantai Yuhuangding Hospital of Qingdao University, Yantai, 264000, PR China

ARTICLE INFO

Keywords:
Fascin2
Cisplatin
Mouse
Ototoxicity
Apoptosis

ABSTRACT

Objectives: Deletion of *Fscn2* gene in mice has been linked to progressive hearing loss and degeneration of cochlear cells. Cisplatin, an antitumor drug, can cause various side effects, including ototoxicity. The aim of this study was to investigate the effects of *Fscn2* on cisplatin-induced hearing impairment in mice and to explore the possible mechanism.
Methods: Two-week-old $Fscn2^{+/+}$ mice and $Fscn2^{-/-}$ mice were treated with two doses of cisplatin, with a 3-day recovery period in between. ABR (auditory evoked brain stem response) thresholds were measured and cochlear pathology was observed at 3 weeks of age.
Results: Both $Fscn2^{+/+}$ and $Fscn2^{-/-}$ mice showed hearing loss under the effect of cisplatin, but the impairment was more severe in $Fscn2^{-/-}$ mice. Further experiments showed that the percentages of outer hair cell (OHC) and spiral ganglion neuron (SGN) loss were significantly higher in cisplatin-treated $Fscn2^{-/-}$ mice compared to $Fscn2^{+/+}$ mice. Additionally, knockdown of *Fscn2* in HEI-OC1 cells worsened cisplatin-induced cell apoptosis.
Conclusion: FSCN2 mediates reduction of CDDP induced ototoxicity by inhibiting cell apoptosis.

1. Introduction

Fascin2 (FSCN2) is a member of the Fascin family. FSCN2 is predominantly found in eye retinas and in hair follicle stereocilia (Hashimoto et al., 2011). Studies on aging deafness mice of DBA/2J have shown that FSCN2 works with β-actin to maintain the length of stereocilia and auditory function (Perrin et al., 2013). To explore the specific role of *Fscn2* in hearing loss, we constructed the Fscn2 knockout mice. C57BL/6J mice with TALEN mutations manifest progressive hearing loss and retinal degeneration (Liu et al., 2018). Additionally, it was found that knockdown of *Fscn2* increased the susceptibility of tubular epithelial cells to cisplatin-induced injury (Wang et al., 2017), indicating that FSCN2 is not only a structural protein, but also plays a role in regulating cell fates.

Cisplatin (cis-diamine dichloroplatinum, CDDP) is a highly effective antitumor drug that is widely used in the treatment of various cancers (Qi et al., 2019). CDDP induces inter- and intrastrand DNA crosslinks, disrupts DNA replication and transcription, and triggers replication stress and DNA damage response (DDR), ultimately leading to cell apoptosis and producing anti-tumor effects (Qi et al., 2019; Pustovalova et al., 2022). However, CDDP can cause various side effects, including nephrotoxicity, neurotoxicity, and ototoxicity (Travis et al., 2014). **Loss of Gsta4 (glutathione transferase α4) in mice results in more profound hearing loss by the treatment with CDDP (Park et al., 2019).**

In this study, we found that lack of FSCN2 in mice increases susceptibility to CDDP-induced hearing impairment and cochlear cell apoptosis.

Peer review under responsibility of PLA General Hospital Department of Otolaryngology Head and Neck Surgery.
* Corresponding author.
** Corresponding author.
E-mail addresses: wenjshang@126.com (W. Shang), hanfengchan@gmail.com (F. Han).
[1] These authors contributed equally to this work.

https://doi.org/10.1016/j.joto.2024.07.001
Received 26 August 2023; Received in revised form 6 June 2024; Accepted 2 July 2024
Available online 19 October 2024

2. Materials and methods

2.1. Mouse preparation and genotyping

Fscn2$^{+/+}$ mice and *Fscn2*$^{-/-}$ mice were developed in our laboratory by Liu et al. (Liu et al., 2018). A total of 116 mice aged three weeks, including 59 *Fscn2*$^{+/+}$ mice and 57 *Fscn2*$^{-/-}$ mice, were bred and housed in a **SPF (specific pathogen free)** animal facility at Binzhou Medical University. The university's institutional Animal Use and Care Committee approved all animal studies (protocol 14–0514). Genotyping of the wild-type mice (*Fscn2*$^{+/+}$) and homozygous knockout mice (*Fscn2*$^{-/-}$) was performed using a polymerase chain reaction (PCR) (Liu et al., 2018), and the images were recorded using a Gel Documentation System (Clinx Science Instruments Co., Ltd, Shanghai, China).

2.2. Treatment in mice with CDDP

Two-week-old mice were divided into four experimental groups and treated with CDDP (purchased from MedChem Express, New Jersey, USA) dissolved in normal saline at 40 °C for 5 min to obtain a 1 mg/mL clear liquid. The drug was injected intraperitoneally at a dosage of 6 mg/kg body weight (Zhang et al., 2020). The mice were allowed to recover for an additional three days before the second dose of CDDP injection.

2.3. ABR threshold tests

At the end of cisplatin administration, the mice were anesthetized with 2% tribromoethanol (0.2 mL per 10 g of body weight) and placed on a heating pad to maintain a temperature of 37 °C. The thresholds of ABR (auditory evoked brain stem response) were measured using the IHSS Smart EP 3.30 and USBez Software (Intelligent Hearing Systems) (Gao et al., 2017).

2.4. Phalloidin staining of outer hair cells (OHCs)

After the ABR tests, the deeply anesthetized mice were sacrificed and the cochleae were collected. Following a previously described method (Liu et al., 2018), the tissues were mounted with glycerin on glass slides, and hair cell bundles were stained with Alexa Fluor-488 conjugated phalloidin (1:500 dilution, Invitrogen, CA, USA). The samples were mounted with VECTASHIELD Mounting Medium H-100 (Vector Laboratories, CA, USA), and examined with a fluorescent microscope (TCS SPE, Leica, Germany).

2.5. Hematoxylin and eosin (HE) staining

After fixation and decalcification, the inner ears were embedded in paraffin. The paraffin-embedded cochlear specimens were sliced into 5 μm sections, stained with hematoxylin and eosin (HE), and observed under a light microscope (BX53, Olympus, Japan). Spiral ganglion neurons were calculated and analyzed in the apical, middle, and basal regions of the cochlear sections using a 40× objective. Counting of spiral ganglion neurons (SGNs) was carried out following the methods described previously (Semaan et al., 2013). A correction factor was determined by dividing the section thickness by the sum of the section thickness plus the mean diameter of the nuclei (Abercrombie and Johnson, 1946; Guillery, 2002). The diameter of nucleus was measured with the aid of Image J software.

2.6. Infection of HEI-OC1 cells with Fscn2-shRNA-lentivirus

HEI-OC1 cells were cultured in Dulbecco's Modified Eagle's Medium (Gibco, USA) at 33 °C in a humidified atmosphere of 10% CO_2. Recombinant plasmids of pGV112-hU6-MCS-CMV-puro-Fscn2 or pGV112-hU6-MCS-CMV-puro-Ctrl were constructed (Shanghai GenePharma, China). These plasmids expressed short hairpin RNA (shRNA) sequences targeting either the mouse *Fscn2* gene or a control sequence. The DNA sequence of *Fscn2*-shRNA was 5′-GCTGGAGTTCAAGGCAGGCAA-3′, while that of the Ctrl-shRNA was 5′-TTCTCCGAACGTGTCACGT-3'.

2.7. Cell proliferation rate tests

Fscn2-shRNA cells and Ctrl-shRNA cells were seeded at an appropriate density and allowed to incubate overnight. The cells were then treated with 30 μM CDDP for 24 h (Zhang et al., 2020). Cell viability was quantified using a commercial Cell Counting Kit-8 (CCK8, C0037, Beyotime Biotechnology, Shanghai, China) according to the manufacturer's instructions. Optical density values were measured at a wavelength of 450 nm (INFINITE 200 PRO, Tecan, Switzerland). The cell survival rate was calculated by dividing the **OD (Optical density)** value of the CDDP-treated cells by the OD value of the CDDP-untreated cells.

2.8. Detection of mitochondrial membrane potential to predict cell apoptosis

Mitochondrial membrane potential was measured using the JC-1 kit (Beyotime, Shanghai, China). The optical density values were measured using the INFINITE 200 PRO (Tecan, Switzerland). To detect JC-1 monomer, the excitation light was set to 490 nm and the emission light to 530 nm. To detect JC-1 polymer, the excitation light was set to 525 nm and the emission light to 590 nm. The ratio of J-aggregates to JC-1 monomers represented the mitochondrial membrane potential (Perelman et al., 2012) and a decrease in mitochondrial membrane potential is one of the markers of cell apoptosis **(Lu et al., 2018)**.

2.9. Western blot for apoptosis-related proteins

To detect apoptosis-related proteins, Western blotting was performed according to previously described protocols (Xu et al., 2020). Briefly, 25 μg of protein was separated by sodium dodecyl sulfate polyacrylamide gel electrophoresis and transferred onto a PVDF membrane, incubation with primary antibodies against FSCN2 (ab232768, 1:400, Abcam), Bcl2 (26593-1-AP, 1:1000, Proteintech), Bax (50599-2-Ig, 1:5000, Proteintech), or cleaved caspase3 (Asp 175) (5A1E) Rabbit mAb (9505, 1:1000, Cell Signaling Technology, USA) overnight at 4 °C. The membrane was then incubated with horseradish peroxidase-conjugated goat anti-rabbit secondary antibody (ab97051, 1:5000, Abcam) for 2 h at room temperature. Protein expression was visualized using the ECL kit (NOVLAND, Shanghai) and detected with a chemiluminescence instrument (Clinx Science Instruments, Shanghai, China). The band intensities were quantified using Image J software.

2.10. RNA extraction and quantitative PCR

Total RNA was extracted from HEI-OC1 cells using TRIzol Reagent (Invitrogen, Carlsbad, CA, USA), followed by reverse transcription using a PrimeScript RT reagent Kit (Roche, Basel, Switzerland) according to the manufacturer's instructions. Quantitative PCR (qPCR) was performed using SYBR Green PCR Master Mix Reagents (Roche, Basel, Switzerland) in the MyiQTM Real-Time PCR Detection System (Bio-Rad Laboratories, Inc., Hercules, CA) with the following primer sequences: *Fscn2* forward, CAGGAAGATGAGATGGCAGCAGAC; *Fscn2* reverse, CCTTGAACTCCAGCGTGTAGCAG; *Gapdh* forward, CTTCCGTGTTCCTACCCCCAATGT; *Gapdh* reverse, GCCTGCTTCACCACCTTCTTGATG.

2.11. Assessment of apoptosis by flow cytometry

Cell apoptosis was measured using an Annexin V-Alexa Fluor 647 Apoptosis Detection Kit (Solarbio Science & Technology, Beijing, China) and analyzed using a BD FACSCantoTMII Flow Cytometer (BD, Franklin Lakes, NJ, USA). About 10,000 cells were measured in each group.

2.12. Statistical analysis

All experiments were repeated at least three times, and data are presented as mean ± S.D. Statistical analysis was performed using SPSS 26 statistical software (IBM). Two-way Repeated Measure ANOVA with Bonferroni's multiple comparison tests were used to evaluate ABR thresholds, as well as OHC and SGN counts. One-way ANOVA with Bonferroni's multiple comparison tests were used to evaluate ABR thresholds at a single frequency or cell counts at a single turn. Other data were analyzed using one-way ANOVA with Bonferroni's multiple comparison tests. $P < 0.05$ was considered statistically significant.

3. Results

3.1. The ABR thresholds were increased more in CDDP treated *Fscn2*$^{-/-}$ mice than in the **CDDP treated *Fscn2*$^{+/+}$** mice at stumulus frequencies of 8 kHz, 16 kHz and click

Intraperitoneal injection of CDDP (6 mg/kg) was given to 2-week-old *Fscn2*$^{+/+}$ and *Fscn2*$^{-/-}$ mice. At 3 weeks of age, auditory brainstem response (ABR) thresholds were obtained for click and pure-tone bursts (8 kHz, 16 kHz, and 32 kHz) stimuli for both untreated and treated mice. Two-way ANOVA (group × frequency) for ABR thresholds between the two groups of mice untreated with CDDP revealed a no significant two-way interaction [F (1, 8) = 4.427, P = 0.069]. In the two groups of mice untreated with CDDP, there was no significant difference in the ABR thresholds between *Fscn2*$^{+/+}$ mice and *Fscn2*$^{-/-}$ mice at the stimulus frequency of 8 kHz [F (1, 18) = 0.043, P = 0.837], or 16 kHz [F (1, 18) = 0.7, P = 0.413]. However, there was a significant difference in the ABR thresholds between *Fscn2*$^{+/+}$ mice and *Fscn2*$^{-/-}$mice at the stimulus frequency of 32 kHz [F (1, 18) = 5.865, P = 0.026] (Fig. 1A). For the mice treated with CDDP, two-way ANOVA (group × frequency) for ABR thresholds showed a significant interaction [F (1, 8) = 16.050, P = 0.004]. The ABR thresholds in *Fscn2*$^{-/-}$ mice were significantly higher than those in *Fscn2*$^{+/+}$ mice for click [F (1, 19) = 4.872, P = 0.04] and pure-tone bursts (8 kHz [F (1, 19) = 24.429, P = 0.000183], 16 kHz [F (1, 19) = 14.43, P = 0.001], and 32 kHz [F (1, 19) = 20.061, P = 0.000257]) (Fig. 1B). The results showed that both *Fscn2*$^{+/+}$ and *Fscn2*$^{-/-}$ mice had hearing loss under the action of CDDP, but the loss was generally more severe in *Fscn2*$^{-/-}$ mice. Therefore, CDDP induced more profound hearing loss in *Fscn2*$^{-/-}$ mice than in the **CDDP treated *Fscn2*$^{+/+}$** mice.

3.2. CDDP caused more OHC loss in *Fscn2*$^{-/-}$ mice than in **CDDP treated *Fscn2*$^{+/+}$ mice**

To investigate the pathology of hearing loss induced by CDDP in *Fscn2*$^{-/-}$ mice, we examined the OHCs in the cochleae of both *Fscn2*$^{+/+}$ and *Fscn2*$^{-/-}$ mice at 3 weeks of age. **In the untreated mice, the OHCs were neatly arranged in both groups (Fig. 2A).** Following treatment with CDDP, both groups exhibited hair cell loss in the cochleae, with irregularly arranged remaining OHCs (Fig. 2B). Two-way ANOVA (group × turns) for percentages of OHC loss in cochleae revealed a significant two-way interaction [F (1, 4) = 198.316516, P = 0.000148]. However, *Fscn2*$^{-/-}$ mice showed significantly higher percentages of OHC loss in the cochlear apical [F (1, 8) = 66.076353, P = 0.000039], middle [F (1, 8) = 235.1534, P = $3.2471*10^{-7}$], and basal turns [F (1, 8) = 41.9844, P = 0.000192] compared to *Fscn2*$^{+/+}$ mice (Fig. 2C). These results demonstrate that CDDP causes more OHC loss in *Fscn2*$^{-/-}$ mice than in *Fscn2*$^{+/+}$ mice, particularly in the cochlear middle turns, which may contribute to the more severe hearing loss observed in *Fscn2*$^{-/-}$ mice.

3.3. The densities of SGNs were reduced more in CDDP treated *Fscn2*$^{-/-}$ mice

SGN densities were evaluated for cochlear sections stained with HE after treatment with CDDP. The cochleae of untreated *Fscn2*$^{+/+}$ and *Fscn2*$^{-/-}$ mice at 3 weeks of age showed complete and evenly distributed SGN structures (Fig. 3A). A two-way ANOVA (group × turns) revealed an insignificant interaction between the groups of untreated mice in terms of SGN densities [F (1, 2) = 0.07134, P = 0.814415]. There was no significant difference in the SGN densities between *Fscn2*$^{+/+}$ and *Fscn2*$^{-/-}$ mice at the cochlear apical [F (1, 4) = 0.001689, P = 0.969186], middle [F (1, 4) = 0.19802, P = 0.335204], or basal turns [F (1, 4) = 1.684211, P = 0.096] (Fig. 3B). However, a significant interaction was observed between the groups of mice treated with CDDP in terms of SGN densities [F (1, 2) = 725.888, P = 0.001375]. The densities of SGNs in the cochlear apical [F (1, 4) = 73.628433, P = 0.001013], middle [F (1, 4) = 24.589561, P = 0.007713], and basal turns [F (1, 4) = 10.278636, P = 0.032712] were more reduced in *Fscn2*$^{-/-}$ mice after treatment with CDDP (Fig. 3C–D).

3.4. Levels of apoptosis-related proteins increased more in the inner ears of CDDP treated *Fscn2*$^{-/-}$ mice

Upon treatment with CDDP, the levels of apoptosis-related proteins were found to increase more significantly in the inner ears of *Fscn2*$^{-/-}$ mice compared to *Fscn2*$^{+/+}$ mice. Bcl-2, which is an indicator of anti-apoptotic protein, exhibited lower expression in the CDDP-treated *Fscn2*$^{-/-}$ mice as compared to the *Fscn2*$^{+/+}$ mice as determined by Western blot analysis (Fig. 4A). On the other hand, Western blot analysis revealed that the levels of Bax and cleaved caspase3, markers of cell apoptosis, were higher in CDDP-treated *Fscn2*$^{-/-}$ mice as compared to *Fscn2*$^{+/+}$ mice (Fig. 4A). Consequently, the ratio of Bcl-2 to Bax was significantly lower in the CDDP-treated *Fscn2*$^{-/-}$ mice than in the

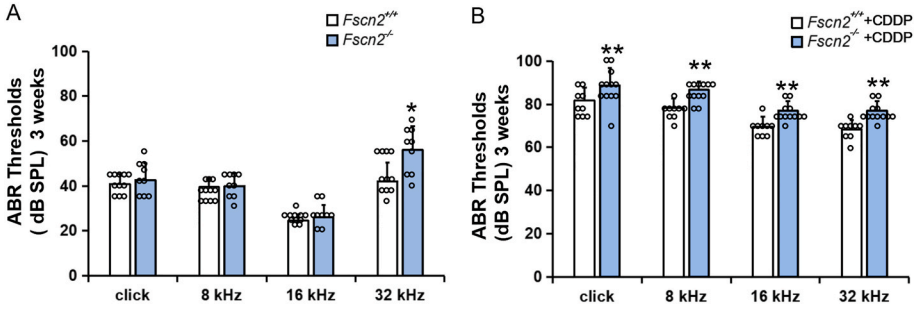

Fig. 1. ABR threshold tests in the 4 mouse groups. Each point represents the mean ABR threshold for one group, with an error bar indicating SD from the mean. The values of the number of individual animals' were overplotted. (n = 11 and 9 for untreated *Fscn2*$^{+/+}$ and *Fscn2*$^{-/-}$ mice; n = 9 and 12 for treated *Fscn2*$^{+/+}$ and *Fscn2*$^{-/-}$ mice, respectively). (A) The results show that at 3 weeks of age, there was no significant difference in the ABR thresholds between the two untreated mouse groups except for 32 kHz. (B) For the CDDP treated mice, ABR thresholds of *Fscn2*$^{-/-}$ mice were significantly higher than that of *Fscn2*$^{+/+}$mice at the stimulation frequencies of click, 8 kHz, 16 kHz and 32 kHz. ABR; auditory-evoked brainstem response; SPL, sound pressure levels; dB, decibel. *$P < 0.05$, **$P < 0.01$.

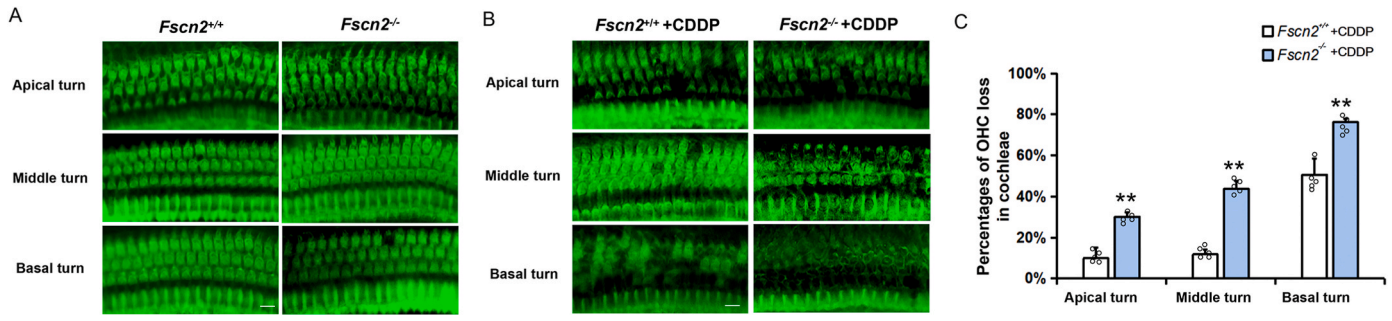

Fig. 2. Observation of OHCs in the mouse cochleae after the treatment with CDDP. (A) Phalloidin labeled OHC of the cochleae of untreated *Fscn2*$^{+/+}$ mice and *Fscn2*$^{-/-}$ mice at 3 weeks of age are shown in green. (B) OHC loss was obvious and cell arrangement was irregular in the CDDP treated *Fscn2*$^{+/+}$ and *Fscn2*$^{-/-}$ mice at 3 weeks of age, especially at the basal turns. (C) Percentages of OHC loss in the 3 turns of cochleae of *Fscn2*$^{+/+}$ and *Fscn2*$^{-/-}$ mice. Scale bar = 10 μm. n = 5 for each group. $^{**}P < 0.01$.

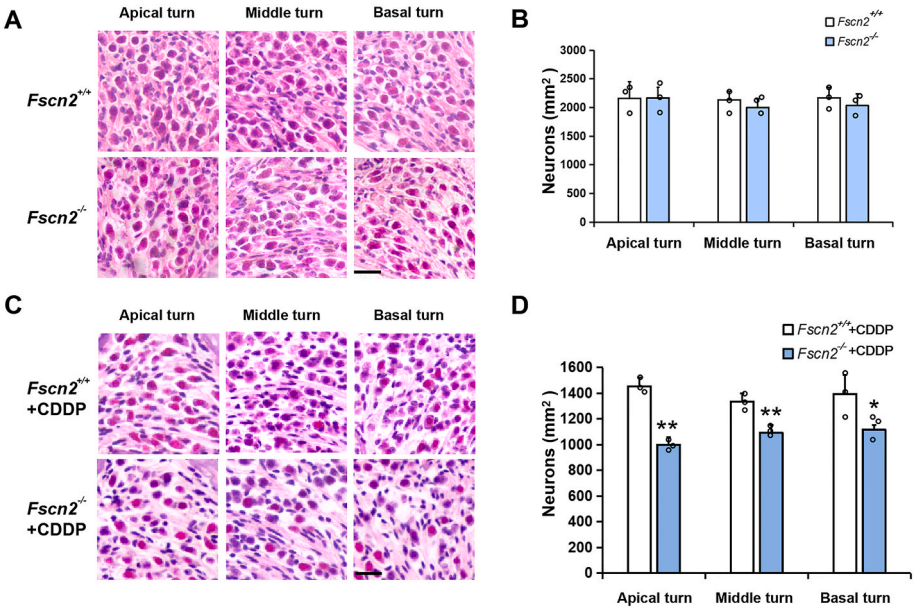

Fig. 3. Evaluation of SGN density by HE staining. (A) SGNs were observed in the cochleae of untreated *Fscn2*$^{+/+}$and *Fscn2*$^{-/-}$ mice at 3 weeks of age. (B) There was no significant difference in the densities of SGNs between the two untreated mouse groups. (C) SGNs were observed in the cochleae of *Fscn2*$^{+/+}$and *Fscn2*$^{-/-}$ mice after the treatment of CDDP. (D) Densities of SGNs in the CDDP treated mice. *Fscn2*$^{-/-}$ mice had fewer SGNs than *Fscn2*$^{+/+}$ mice in the apical, middle and basal turns. Scale bar = 20 μm.n = 3 for each group. $^{*}P < 0.05$; $^{**}P < 0.01$.

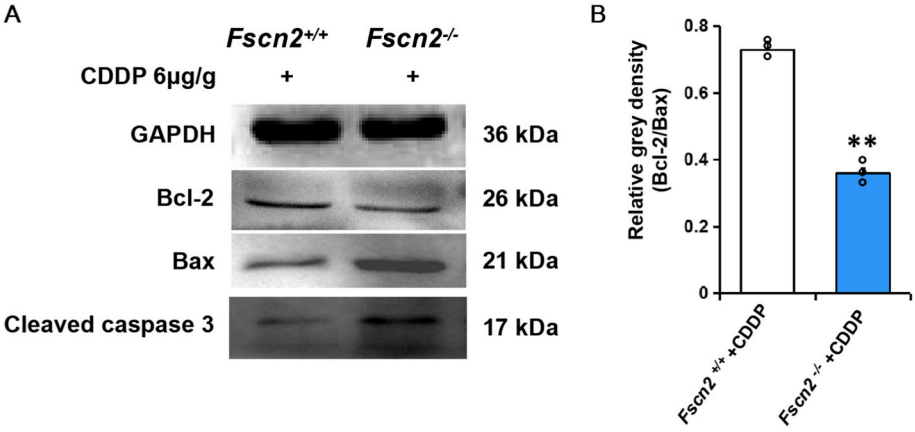

Fig. 4. Expression of Bax, Bcl-2 and cleaved caspase3 in the inner ears of *Fscn2*$^{-/-}$ mice after the treatment with CDDP. (A) Levels of Bax, Bcl-2 and cleaved caspase3 were detected in the inner ears of *Fscn2*$^{+/+}$ and *Fscn2*$^{-/-}$ mice by Western blot. (B) Cell apoptosis was evaluated by calculating the ratio of relative gray densities of Bcl2/Bax. n = 3 for each group. $^{*}P < 0.01$.

Fscn2$^{+/+}$ mice [F (1, 4) = 557.797, p = 0.000019] (Fig. 4B). These findings indicate that the pathological changes induced by CDDP in the inner ears of *Fscn2*$^{-/-}$ mice are associated with an increase in apoptosis.

3.5. Apoptotic cells were increased in the Fscn2-shRNA infected HEI-OC1 cells after the treatment with CDDP

FSCN2 expression level in HEI-OC1 cells was determined by qRT-PCR and Western blot (Fig. 5A and B). The results showed that FSCN2 expression was decreased in HEI-OC1 cells infected with LV-Fscn2-shRNA (*Fscn2*-shRNA cells), compared to the cells infected with LV-Ctrl-shRNA (Ctrl-shRNA cells). At 24 h after the treatment with 30 μM CDDP, the proliferation activity of *Fscn2*-shRNA cells was significantly lower than that of the Ctrl-shRNA cells [F (1, 5) = 748.638, p = 0.0001] (Fig. 5C). A declined mitochondrial membrane potential is one of the markers of early cell apoptosis. As a result, mitochondrial membrane potential of *Fscn2*-shRNA cells was declined after the treatment with CDDP [F (1, 6) = 18.134, P = 0.005331] (Fig. 5D), indicating an increasing percentage of early apoptotic cells. Furthermore, Annexin V/Alexa Fluor 647 was used to label the cells undergoing apoptosis and propidium iodide to label the dead cells. After the treatment with CDDP, the ratios of apoptotic cells were significantly increased compared to the Ctrl-shRNA cells [F (1, 7) = 22.386, p = 0.002] (Fig. 5E–F).

3.6. The levels of apoptosis-related proteins were increased more in Fscn2-shRNA infected cells after the treatment with CDDP

After treatment with CDDP, *Fscn2*-shRNA cells showed a lower expression level of Bcl-2 compared to Ctrl-shRNA cells, as demonstrated by Western blot analysis (Fig. 6A). Additionally, *Fscn2*-shRNA cells exhibited a higher expression level of cleaved caspase3 compared to Ctrl-shRNA cells (Fig. 6A). The ratio of Bcl-2 to Bax in *Fscn2*-shRNA cells was also lower than that of Ctrl-shRNA cells [F (1, 4) = 24.208, p = 0.008] (Fig. 6B), indicating that the knockdown of *Fscn2* may enhance apoptosis in cells treated with CDDP.

4. Discussion

4.1. Loss of FSCN2 exacerbates CDDP-induced hearing impairment in mice

Mouse models are essential for studying the pathogenesis associated with gene variants (Angeli et al., 2012). In our laboratory, we developed a *Fscn2*$^{-/-}$ mouse strain that exhibits early onset (3 weeks) progressive hearing loss to investigate the role of *Fscn2* (Liu et al., 2018). Studies have revealed that gene variants are associated with cisplatin-related ototoxicity (Travis et al., 2014; Park et al., 2019; Wheeler et al., 2017). For instance, CDDP has been shown to cause more severe hearing loss in some gene knockout mice. In our study, 2-week-old mice were

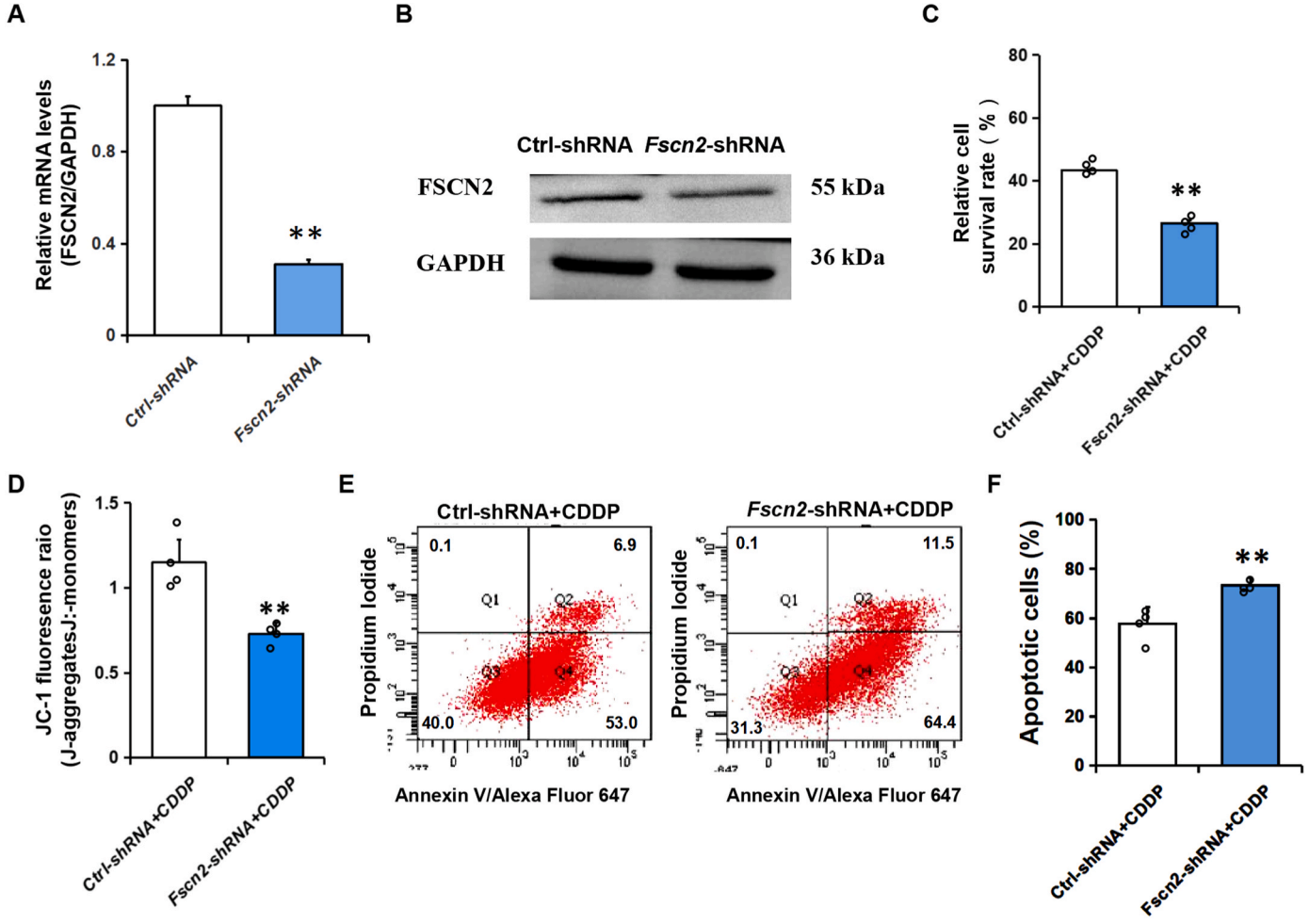

Fig. 5. Proliferation rate and apoptotic ratio of HEI-OC1 cells with low *Fscn2* expression. (A–B) Evaluation of mRNA levels with RT-PCR and FSCN2 levels by Western blot in Ctrl-shRNA infected cells (Ctrl-shRNA) and *Fscn2*-shRNA infected cells (*Fscn2*-shRNA). (C) Cell proliferation rate was measured by CCK-8 assay after the treatment with 30 μM CDDP for 24 h. (D) Cell apoptosis was evaluated by JC-1 assay. A decrement in the ratio of J-aggregates to J-monomers is an indicator of early cell apoptosis. (E–F) Flow cytometry was used to detect apoptotic cells exposed to 30 μM CDDP for 24 h n = 4 for each group. *$P < 0.05$; **$P < 0.01$.

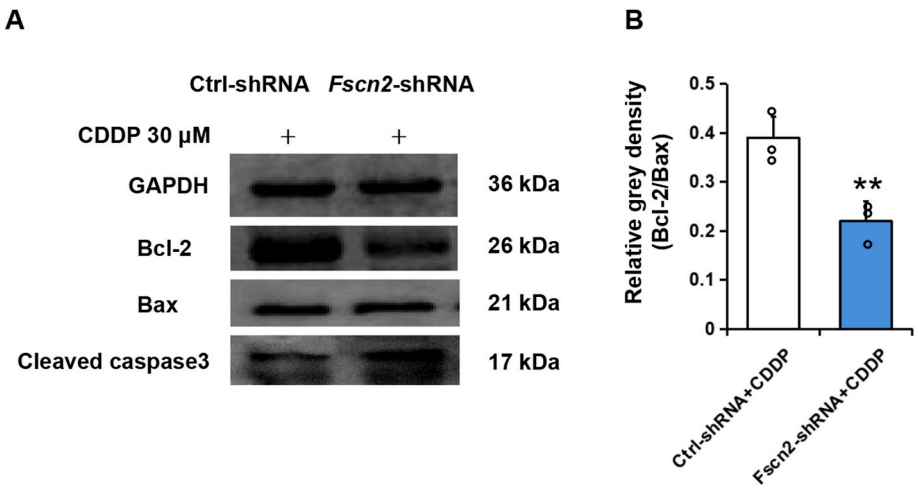

Fig. 6. Expression of apoptosis-related proteins in *Fscn2*-shRNA infected cells after the treatment with CDDP. (A) Levels of Bcl-2, Bax and cleaved caspase3 were detected by Western blot. (B) The ratio of Bcl-2 to Bax represents the relative gray density of the two proteins in Western blot in Ctrl-shRNA infected cells (Ctrl-shRNA) or in *Fscn2*-shRNA infected cells (*Fscn2*-shRNA). n = 3 for each group. $^{*}P < 0.01$.

selected for the experiments as there was a significant difference in the ABR thresholds at a stimulus frequency of 32 kHz between the $Fscn2^{-/-}$ and $Fscn2^{+/+}$ groups at 3 weeks of age. As a result, we found that $Fscn2^{-/-}$ mice at 3 weeks of age exhibited more severe hearing impairment than $Fscn2^{+/+}$ mice after treatment with CDDP (Fig. 1). Since the *Fscn2* gene is the only different component between $Fscn2^{-/-}$ and $Fscn2^{+/+}$ mice, our results suggest that FSCN2 functions to reduce the ototoxicity of CDDP in juvenile mice.

4.2. FSCN2 functions to maintain cochlear cell integrity

Age-related hearing loss is primarily characterized by the degeneration of cochlear cells, including hair cells, spiral ganglion neurons, and stria vascularis (Yamasoba et al., 2013). $Fscn2^{-/-}$ mice show progressive loss of outer hair cells (OHCs) (Liu et al., 2018) and spiral ganglion neurons (SGNs) **(Liu et al, 2024)**. In mice, gene deletions or mutations exacerbate the ototoxic effects of CDDP. In this study, we found that CDDP treatment led to significantly increased loss of OHCs and SGNs in the cochlear basal turns of $Fscn2^{-/-}$ mice compared to CDDP-treated $Fscn2^{+/+}$ mice (Figss. 2 and 3). There were no significant differences in the loss of OHCs and SGNs between untreated $Fscn2^{+/+}$ and $Fscn2^{-/-}$ mice at 3 weeks of age. These results suggest that $Fscn2^{-/-}$ mice are more vulnerable to the insults of CDDP, leading to greater cochlear cell damage.

4.3. FSCN2 mediates reduction of CDDP induced ototoxicity by inhibiting cell apoptosis

Studies have demonstrated that the expression of apoptosis-related proteins, such as cleaved caspase3, is increased in response to CDDP treatment (Zhang et al., 2020). In a separate study, overexpression of *Fscn2* gene attenuated the increased susceptibility of C2 cells to cisplatin-induced injury (Wang et al., 2017). To investigate whether the loss of *Fscn2* exacerbates CDDP ototoxicity through apoptosis, we found that the levels of Bax and cleaved caspase3 were higher, while the Bcl-2 to Bax ratio was lower in the cochleae of CDDP-treated $Fscn2^{-/-}$ mice (Fig. 4). In vitro studies using *Fscn2* knockdown HEI-OC1 cells showed that apoptotic cells and apoptosis-related protein levels increased after CDDP treatment (Figss. 5 and 6). Moreover, our recent study showed that overexpression of FSCN2 in HEI-OC1 cells inhibited cisplatin-induced apoptosis (Wang et al., 2022). These findings suggest that $Fscn2^{-/-}$ mice and *Fscn2*-shRNA cells are more susceptible to CDDP-induced cochlear cell apoptosis.

In conclusion, our results indicate that the loss of *Fscn2* leads to the intensification of CDDP-induced ototoxicity and greater cochlear cell damage. FSCN2 mediates the reduction of CDDP-induced ototoxicity by inhibiting cell apoptosis.

Ethics approval

We promise that in all animal experiments, we care and protect animals without unnecessary harm. All experimental operations strictly followed the 'The Basel Declaration' and 'International Council for Laboratory Animal Science (ICLAS) has been published ethical guidelines'.

The mice were bred in the SPF animal breeding center of Binzhou Medical University. At the end of the animal surgery, we euthanized the mice according to the instructions of the "American Veterinary Medical Association (AVMA) Guidelines for the Euthanasia of Animals (2020)" (Leary et al., 2020). All of the experimental protocols in this study were approved by the Animal Research Ethics Committee of Binzhou Medical University.

Funding

This project was supported by the National Natural Science Foundation of China (No. 81771020, 81570927 and 81271092), and Grant for Scientific and Technological Development Plan for Medical and Health in Shandong Province (2019WS341).

Declaration of competing interest

The authors report no conflicts of interest. The authors alone are responsible for the content and writing of the paper.

Acknowledgments

Fengchan Han, Wenjing Shang and Yan Sun conceived and designed the experiments. Yan Wang, Yingying Liu, Yi Xie, Jun Luan, Rongrong Liu, Yongjia Zhu, Ying Ma, Yi Fan, Yan Sun, Wenjing Shang and Fengchan Han performed the experiments and analyzed the data. Yan Wang and Fengchan Han wrote the paper.

References

Abercrombie, M., Johnson, M.L., 1946. Quantitative histology of Wallerian degeneration: I. Nuclear population in rabbit sciatic nerve. J. Anat. 80, 37–50.

Angeli, S., Lin, X., Liu, X.Z., 2012. Genetics of hearing and deafness. Anat. Rec. 295, 1812–1829.
Gao, L., Ge, R., Xie, G., Yao, D., Li, P., Wang, O., Ma, X., Han, F., 2017. Hearing improvement in A/J mice via the mouse nerve growth factor. Clin Exp Otorhinolaryngol 10, 303–308.
Guillery, R.W., 2002. On counting and counting errors. J. Comp. Neurol. 447, 1–7.
Hashimoto, Y., Kim, D.J., Adams, J.C., 2011. The roles of fascins in health and disease. J. Pathol. 224, 289–300.
Leary, S., Underwood, W., Anthony, R., Cartner, S., Grandin, T., Greenacre, C., Gwaltney-Brant, S., McCrackin, M.A., Meyer, R., Miller, D., Shearer, J., Turner, T., Yanong, R., Johnson, C.L., Patterson-Kane, E., 2020. AVMA Guidelines for the euthanasia of animals: 2020 Edition. Schaumburg: American Veterinary Medical Association, 2020.
Liu, X., Zhao, M., Xie, Y., Li, P., Wang, O., Zhou, B., Yang, L., Nie, Y., Cheng, L., Song, X., Jin, C., Han, F., 2018. Null mutation of the fascin2 gene by TALEN leading to progressive hearing loss and retinal degeneration in C57BL/6J mice. G3 (Bethesda). 8, 3221–3230.
Liu, R., Shang, W., Liu, Y., Xie, Y., Luan, J., Zhang, T., Ma, Y., Wang, Z., Sun, Y., Song, X., Han, F., 2024. Inhibition of the ILK-AKT pathway by upregulation of PARVB contributes to the cochlear cell death in Fascin2 gene knockout mice. Cell death discovery 10 (1), 89.
Lu, J., Wu, L., Wang, X., Zhu, J., Du, J., Shen, B., 2018. Detection of mitochondria membrane potential to study CLIC4 knockdown-induced HN4 cell apoptosis in vitro. J. Vis. Exp. (137), 56317
Park, H.J., Kim, M.J., Rothenberger, C., Kumar, A., Sampson, E.M., Ding, D., Han, C., White, K., Boyd, K., Manohar, S., Kim, Y.H., Ticsa, M.S., Gomez, A.S., Caicedo, I., Bose, U., Linser, P.J., Miyakawa, T., Tanokura, M., Foster, T.C., Salvi, R., Someya, S., 2019. GSTA4 mediates reduction of cisplatin ototoxicity in female mice. Nat. Commun. 10, 4150.
Perelman, A., Wachtel, C., Cohen, M., Haupt, S., Shapiro, H., Tzur, A., 2012. JC-1: alternative excitation wavelengths facilitate mitochondrial membrane potential cytometry. Cell Death Dis. 3 (11), e430.
Perrin, B.J., Strandjord, D.M., Narayanan, P., Henderson, D.M., Johnson, K.R., Ervasti, J. M., 2013. Beta-Actin and fascin-2 cooperate to maintain stereocilia length. J. Neurosci. 33, 8114–8121.
Pustovalova, M., Blokhina, T., Alhaddad, L., Chigasova, A., Chuprov-Netochin, R., Veviorskiy, A., Filkov, G., Osipov, A.N., Leonov, S., 2022. CD44+ and CD133+ Non-Small cell lung cancer cells exhibit DNA damage response pathways and dormant polyploid giant cancer cell enrichment relating to their p53 status. Int. J. Mol. Sci. 23.
Qi, L., Luo, Q., Zhang, Y., Jia, F., Zhao, Y., Wang, F., 2019. Advances in toxicological research of the anticancer drug cisplatin. Chem. Res. Toxicol. 32, 1469–1486.
Semaan, M.T., Zheng, Q.Y., Han, F., Zheng, Y., Yu, H., Heaphy, J.C., Megerian, C.A., 2013. Characterization of neuronal cell death in the spiral ganglia of a mouse model of endolymphatic hydrops. Otol. Neurotol. 34, 559–569.
Travis, L.B., Fossa, S.D., Sesso, H.D., Frisina, R.D., Herrmann, D.N., Beard, C.J., Feldman, D.R., Pagliaro, L.C., Miller, R.C., Vaughn, D.J., Einhorn, L.H., Cox, N.J., Dolan, M.E., 2014. Chemotherapy-induced peripheral neurotoxicity and ototoxicity: New paradigms for translational genomics. J. Natl. Cancer Inst. 106.
Wang, X., Nichols, L., Grunz-Borgmann, E.A., Sun, Z., Meininger, G.A., Domeier, T.L., Baines, C.P., Parrish, A.R., 2017. Fascin2 regulates cisplatin-induced apoptosis in NRK-52E cells. Toxicol. Lett. 266, 56–64.
Wang, Y., Shang, W., Han, F., 2022. Overexpression of Fscn2 Inhibits Cisplatin-Induced Apoptosis of Cochlear Cells, vol. 45. The Journal of Binzhou Medical University, pp. 17–20.
Wheeler, H.E., Gamazon, E.R., Frisina, R.D., Perez-Cervantes, C., El, C.O., Mapes, B., Fossa, S.D., Feldman, D.R., Hamilton, R.J., Vaughn, D.J., Beard, C.J., Fung, C., Kollmannsberger, C., Kim, J., Mushiroda, T., Kubo, M., Ardeshir-Rouhani-Fard, S., Einhorn, L.H., Cox, N.J., Dolan, M.E., Travis, L.B., 2017. Variants in WFS1 and other mendelian deafness genes are associated with Cisplatin-Associated ototoxicity. Clin. Cancer Res. 23, 3325–3333.
Xu, A., Shang, W., Wang, Y., Sun, X., Zhou, B., Xie, Y., Xu, X., Liu, T., Han, F., 2020. ALA protects against ERS-mediated apoptosis in a cochlear cell model with low citrate synthase expression. Arch. Biochem. Biophys. 688, 108402.
Yamasoba, T., Lin, F.R., Someya, S., Kashio, A., Sakamoto, T., Kondo, K., 2013. Current concepts in age-related hearing loss: epidemiology and mechanistic pathways. Hear. Res. 303, 30–38.
Zhang, W., Xiong, H., Pang, J., Su, Z., Lai, L., Lin, H., Jian, B., He, W., Yang, H., Zheng, Y., 2020. Nrf 2 activation protects auditory hair cells from cisplatin-induced ototoxicity independent on mitochondrial ROS production. Toxicol. Lett. 331, 1–10.